Phenology NEON Forecast Challenge

Logan Monks, Cazimir Kowalski, Keo Pangan, and Miriam Grady

Introduction

Trees invest stored carbon into leaves that are used to capture sunlight and carbon dioxide for use in the photosynthetic pathway of energy production. The growth and senescence of these leaves and their timing is known as leaf phenology. In temperate forests, the timing of these events happens on a seasonal basis, as trees maximize their ability to gain carbon during the summer months that make up the growing season. Thus, leaf budding and growth typically occur in the spring, while leaf senescence occurs during autumn. Temperate trees biologically induce leaf budding in the spring to avoid exposure to cold temperatures that would damage or kill newly produced leaves. Similarly, trees induce leaf senescence in order to resorb some of the available nutrients in the leaf prior to prolonged exposure to freeze / thaw temperature cycles that induce air blockages in the trees' vasculature that would result in leaf death. In other words, the major driver of temperate leaf phenology is a balance of carbon gain through photosynthesis and carbon loss due to xylem embolism induced leaf death. Thus, a large amount of research has concluded that exposure to different temperature thresholds signal trees to begin leaf production and senescence. Additionally, the amount of photosynthetically available radiation is further used by trees to avoid having their biological strategy being dependent on abnormal temperature patterns that may occur (e.g. an unusually warm period in autumn as experienced this year).

Leaf phenology is monitored daily by canopy cameras deployed by the phenocam network. Individual pixels from the canopies of trees are selected, and analyzed for greenness, known as green chromatic coordinate (gcc, see equation 1). The National Ecological Observatory Network (NEON) has collaborated with the phenocam network to get daily images of the canopies in their field sites. This high resolution phenological data provides an excellent opportunity to produce near term forecasts of phenology across a range of forest sites.

Eq. 1: $$G_{CC} = GdnGdn + Bdn + Rdn$$

Interest in forecasting phenology is primarily driven by its critical importance to carbon, water, and energy fluxes. However, phenology remains a poorly understood process within ecosystem models. Thus forecasting phenology has both an applied goal of being able to more accurately forecast and model ecosystem fluxes, while also being a useful research tool that can be used to test hypotheses about the processes controlling phenology by comparing forecast predictions with future observations. Additionally, the use of a bayesian forecasting framework enables researchers to account for many sources of uncertainty and partition and propagate uncertainty in near term forecasts. Analyses of the uncertainty can then be used to determine where our forecasts and thus understanding of processes that control phenology can be improved. Forecasting phenology also provides a unique challenge due to annual differences in weather patterns that lead to differences in the timing of leaf phenological events as well as the directional changes in the timing of these events associated with global climate change.

The goal of our project was to create a near term forecast of leaf phenology, measured as gcc, as a function of one climatic driver. Our aim was to determine if adding a climatic driver made our forecast more accurate and reduced uncertainty in the forecast. To accomplish our goal, we created four models to compare with one another: a null random walk model, a climate driver model, a random walk and climate driver model, and a random walk, climate driver, and endogenous variable model. We then propagated and partitioned uncertainty in order to analyze ways that our models perform and could be improved.

Data

The NEON Forecast Challenge established by the Ecological Forecasting Initiative provides access to phenocam data, site metadata, and past and future weather forecast data. We decided to focus our study on UNDERC, Harvard Forest, SERC, and the Great Smoky Mountain NEON sites since they are natural temperate deciduous forests that comprise a variety of climates within the temperate zone of North America. We used only phenocam data from the period that past climate data was available from NOAA, to prevent differences in the calibration of our different models due to differences in data that was included. Observed data ranges from September 25, 2020 to the date a forecast is run and is forecasted daily for 34 days into the future.

The peak in gcc appears to align more closely with the peak in shortwave radiation (figure 1), whereas temperature keeps increasing through the summer even as gcc declines. For this reason we have chosen to use shortwave radiation as our single climatic driver of gcc, although we acknowledge this does not perfectly reflect the biology of leaf phenology.

Model description

Overview

All models were based on the Bayesian Hierarchical Model simulator JAGS (Plummer, 2003) and executed in R (R Core Team, 2022). Each of the models contained site random effects to account for unmeasured climatic drivers, edaphic drivers, or species composition differences between sites.

Random walk model

To start, the first model generated was a random walk model. The purpose of this was to create a model that could be compared to our other models to determine if the inclusion of daily short wave radiation reduced the uncertainty in our forecast and improved the predictability of our model. For a random walk model, today’s gcc index is dependent on a stochastic draw from a normal distribution of yesterday’s gcc index.

Eq 2: mu[t,s]=x[t-1,s]+ site[s]

Climatic driver only

The second model we created was a climatic driver (CD) only model. The purpose of this model was to understand how well gcc can be forecasted without a dependence on the most recent phenological conditions. We expect that this model will show high uncertainty in its predictions for past data and forecasted data since it could depend on fluctuations in shortwave radiation that may occur daily due to cloud cover. However, we still feel it will be useful to compare this with the models that are dependent on recent phenological conditions.

Eq 3: mu[t,s]=1Driver[t,s] +site[s]

Climatic driver and random walk (state-space)

For our third model, we combined our first two models into a random walk model with the addition of a climatic driver (RWCD). In this model today's gcc is dependent on yesterday's gcc, a site random effect, and the climatic driver parameter multiplied by the daily mean of shortwave radiation. We expect that this model will show better predictive ability when compared with both the RW and CD only models since the process is constrained by yesterday's gcc such that a day with high gcc should not be followed by a day with low gcc, while also containing a temperature driver that will provide an expected directional change for gcc according to cyclical changes in shortwave radiation that share similarities with seasonal changes in gcc.

Eq 4: mu[t,s]=x[t-1,s]+ 1Driver[t,s] + site[s]

Climatic driver and random walk (state-space) and endogenous variable

Our last model was built off the RWCD model with the addition of an endogenous variable. Thus today's gcc is dependent on yesterday's gcc plus today's shortwave radiation and a parameter that describes a change in gcc according to yesterday's gcc value. This model was developed with an aim to make it so that the model could predict positive or negative changes in gcc according to its current value.

Eq 5: mu[t,s]=x[t-1,s]+ 1Driver[t,s] +2 x[t-1,s] + site[s]

Sources of uncertainty

Our model contained process uncertainty, observation uncertainty, and parameter uncertainty. Observation uncertainty in gcc was calculated by finding the standard deviation in gcc indices captured from images on each day of phenocam data collection.

Model calibration

Each of the models was calibrated using data starting from September 25, 2020 to the day prior to the day a forecast is made. For example, a forecast made on December 15, 2022 would be based upon a calibrated model of data from September 25, 2020 to December 14, 2022. The models were run using *rjags* with a burn in period of 1000 iterations. The models were then run for 3000 iterations. We used the posterior estimates of gcc to create time-series visualization of predicted gcc, observed gcc and 95% credible intervals of gcc (figures 3 and 4). After the burn in period the chains were well converged except in the model that included a parameter for an endogenous effect on phenology (figure 2). Due to the failure to converge we did not analyze posterior results from this model or use the posterior means to forecast gcc into the future.

Forecast and Uncertainty Propagation

We saved posterior estimates of gcc, the site level random effect parameter, the beta parameter for shortwave radiation drivers, process precision, and random site effect precision for use in to forecast gcc into the future. To deterministically forecast gcc, the posterior means for each of the model parameters, initial conditions (final day of the calibrated model), and forecast ensembles of shortwave radiation into a linear equation. As an example the random walk model with shortwave radiation as a driver would calculate gcc on day 1 of the forecast to be a function of mean posterior gcc for the last day of the calibrated model plus the posterior mean for the driver parameter multiplied by the mean value for forecasted shortwave radiation and the associated site level parameter.

Forecasts were run for 34 days and sources of uncertainty were added incrementally in order to propagate and partition uncertainty across different lengths of the forecast. Specifically, uncertainty in initial conditions, model parameters, process, drivers, and across sites was propagated into the forecast. Two thousand random draws were taken from the posterior distributions for process precision, initial conditions (final day of the calibrated model), model parameters, and differences across sites to create 2000 different forecasts. Uncertainty was then visualized across the 34 day forecast using 95% credible intervals (see figure blank), while uncertainty was partitioned on a relative contribution scale that ranged from zero to one (see figure blank).

The forecasts appear to accurately predict the direction of gcc change over the 34 forecasted days, given that gcc appears to remain constant as is expected during the winter months in which there are no deciduous leaves on the trees. In the RW and RWCD with shortwave radiation as a driver forecasts, uncertainty is low to begin with (figure 5), but increases as the forecasts progress. For example, the higher end of the 95% credible interval of gcc at UNDERC takes values near 0.37, which are typically only seen during spring green up or leaf senescence, not winter periods. Propagated uncertainty at each of the sites begins with a high importance of initial conditions owing to the nature of a random walk being dependent on the previous data point (figure 5 and 6). The greatest importance of initial condition uncertainty is present at SERC. This is likely caused by the phenocam data that was missing leading up to the forecast. As the RW and RWCD forecasts progress, process uncertainty increases and begins to take a dominant role in overall forecast uncertainty. Across all the models RW, RWCD, and CD, the parameter uncertainty does not play a significant role in forecast uncertainty (figure 5 and 6). Surprisingly driver uncertainty does not play a significant role in the RWCD model or the CD model (figure 5 and 6). One possible explanation is that there is not generally a large amount of variability in forecast ensembles for shortwave radiation at this time of the year. Another, and perhaps more likely explanation is that process uncertainty is so high in the forecast that the exact value of a driver and thus driver uncertainty does not have a huge impact on the forecast. Interestingly, out of site forecasts show relatively little uncertainty in both the RW and RWCD models, while out of site predictions in the CD only forecast show extreme uncertainty to the extent nearly all possible gcc values are contained within the 95% credible interval. This has apparently arisen because the uncertainty of the site random effects in the calibrated CD only model are two orders of magnitude larger than they were in the RW and RWCD models.

Discussion

Overall our models were able to predict the expected lack of directional change in gcc over the course of the 34 days. However, it is unclear whether this ability to predict the directional change in gcc over the 34 days only occurs because of the time of year the forecast was made. It should be easier for random walk models to predict a relatively flat trendline that is seen in gcc during this time of year. Future work should consider hindcasting gcc during different times of the year in which gcc is changing positively during spring leaf budding and growth and changing negatively during autumn leaf senescence.

Both the RW and RWCD models were characterized by growing model uncertainty, while the CD model showed a similar level of very high uncertainty across the entire forecast. In all models, process uncertainty was the major contributor to overall forecast uncertainty. High model process uncertainty is relatively easily explained by the reliance on a random walk model. Additionally, in the models that contain a climatic driver (CD and RWCD), process uncertainty still appears to be high. This was not unexpected, since previous research has demonstrated that there are multiple climatic drivers of leaf phenology. Furthermore, these drivers are probably more accurately represented by non-linear thresholds which signal leaf budding, growth, and senescence instead of a direct dependence of phenological measurements (e.g. gcc) on climatic drivers. Additionally, the research communities' understanding of the internal and external processes governing leaf phenology are incomplete.

Our model demonstrates that an improved forecast is largely dependent upon improving the process model. To accomplish this future forecasts would potentially benefit from not modeling gcc as a linear process that is dependent on climate drivers. Instead a non-linear model with lagged effects for climate may improve the model performance. Additionally, previous phenology research suggests that the amount and timing of late summer and autumn precipitation events can influence leaf color during autumn senescence. This highlights further challenges associated with forecasting phenology since color during senescence and budding are determined by different climatic drivers and thresholds. Thus, one possible improvement could be determining how to appropriately model an endogenous control on leaf phenology. Our model that attempted to use an endogenous parameter did not converge. This is likely because we modeled this as a linear process and thus a single parameter value should have been chosen across a range of gcc values. This is clearly flawed since at both high and low gcc values, the directional change should be negligible, but at intermediate values of gcc the directional change will be larger and would be positive in spring and negative in autumn. Instead, this endogenous factor might be better modeled as a form of temporal autocorrelation that can take into account that today's gcc should be more similar to yesterday's gcc than it is to the gcc seven days earlier.

References

Dietze, Michael C. (2017). *Ecological Forecasting*. Princeton University Press.

Ecological Forecasting Initiative. (2022). *Theme: Phenology*. Ecological Forecasting Initiative. Retrieved from: https://projects.ecoforecast.org/neon4cast-docs/Phenology.html

Figures

Figure 1: Seasonal changes in phenology, sunlight, and temperature as measured by gcc, shortwave radiation and degrees celsius. All three variables exhibit seasonal cycles that differ according to the plot. The peak in phenology (green) aligns more closely with shortwave radiation (yellow) than it does with mean air temperature (blue).

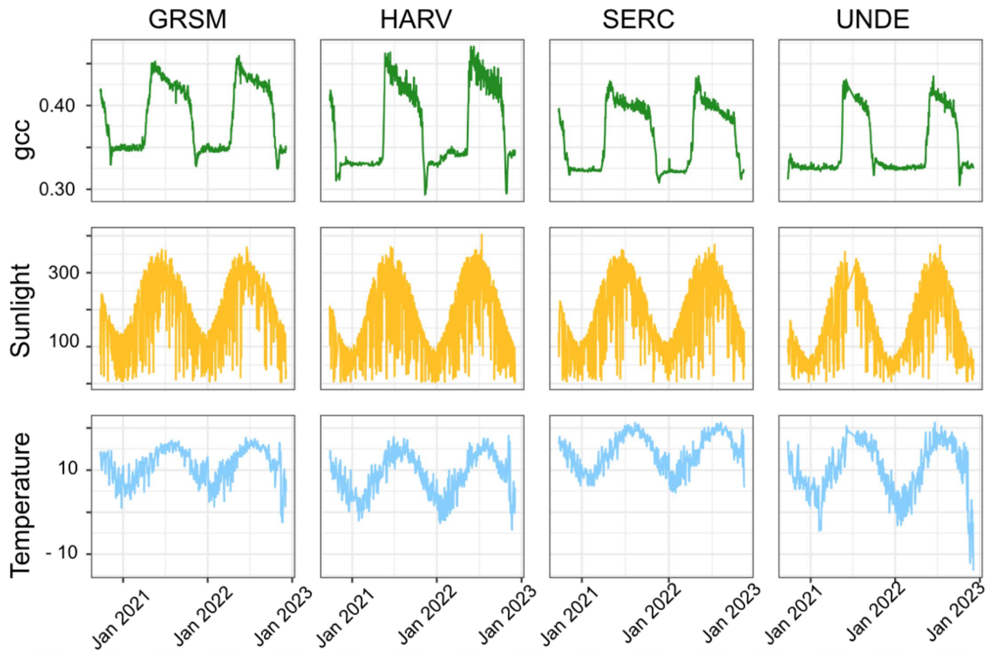

Figure 2: Example trace plots from the RWCD model and RWCD + endogenous variable model.

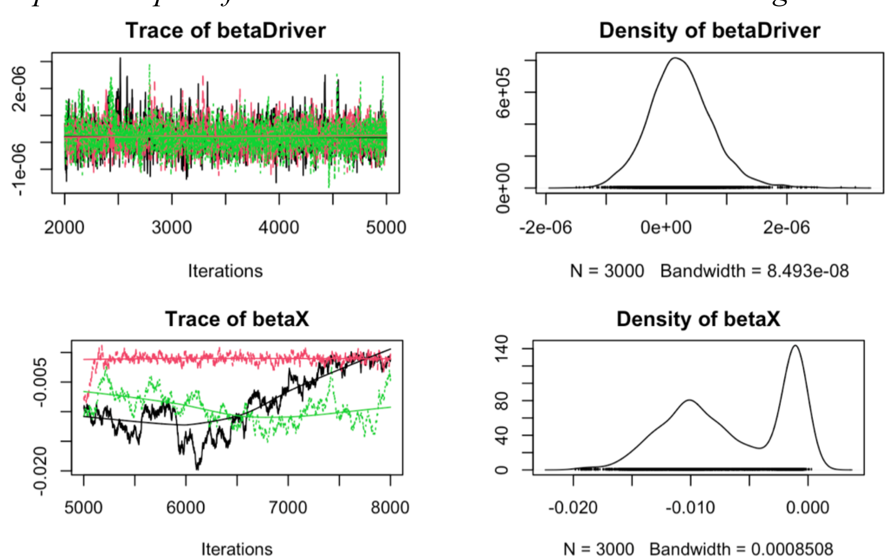

Figure 3: Observed and predicted gcc from RWCD model.

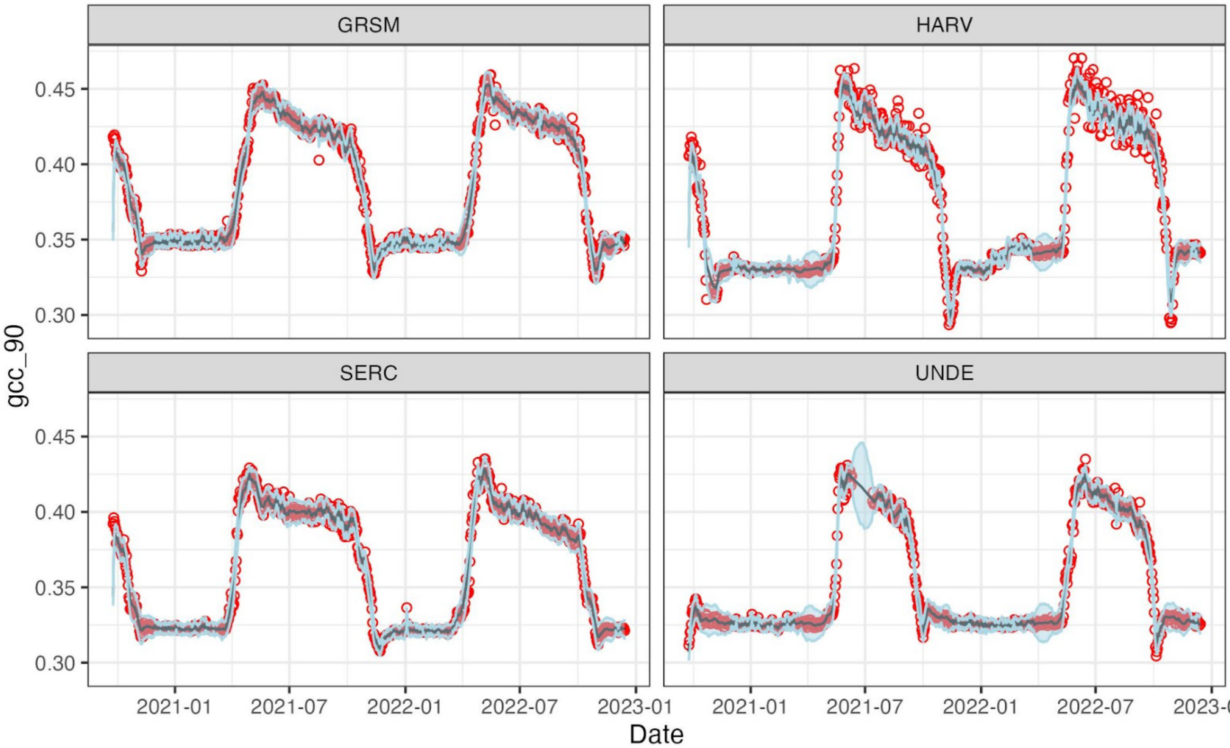

dFigure 4: 95% credible intervals for RW, RWCD, and CD models.

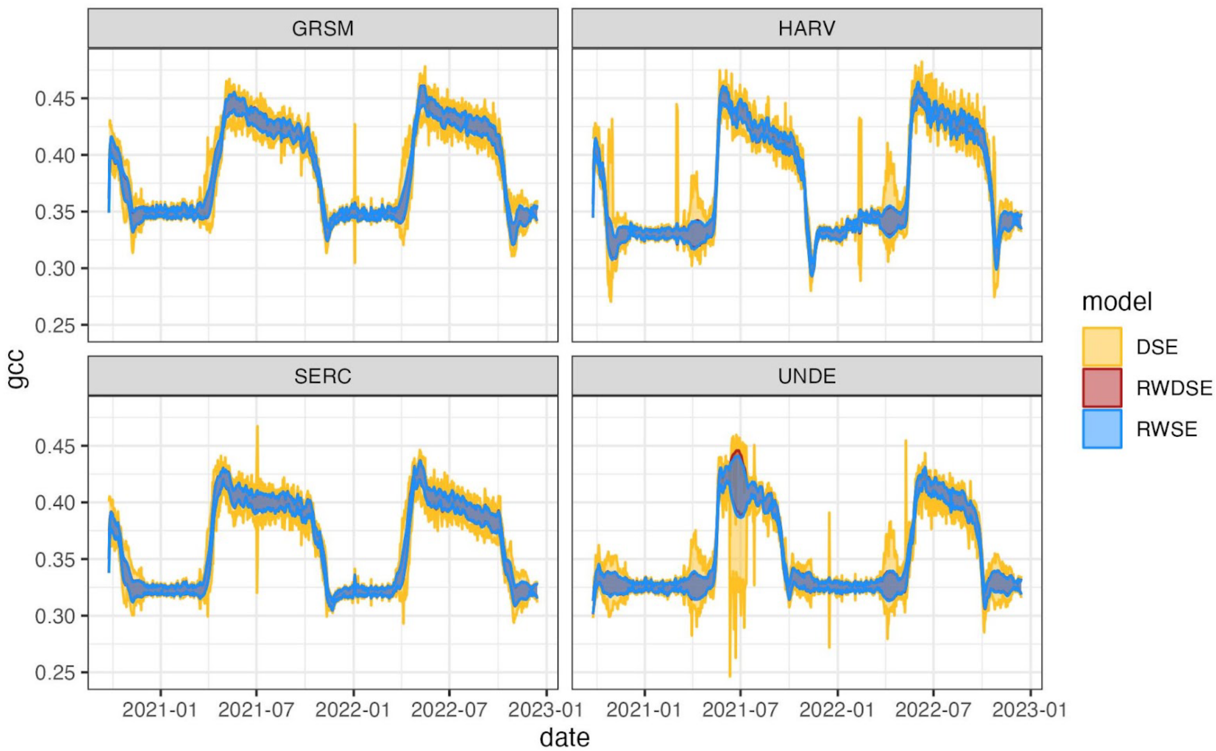

Figure 5: Propagated uncertainty of RWCD forecast (left) and CD forecast (right) for UNDERC. Light blue represents initial condition uncertainty, red represents parameter uncertainty, yellow represents driver uncertainty, bluish purple represents process uncertainty and reddish purple represents out of site prediction uncertainty.

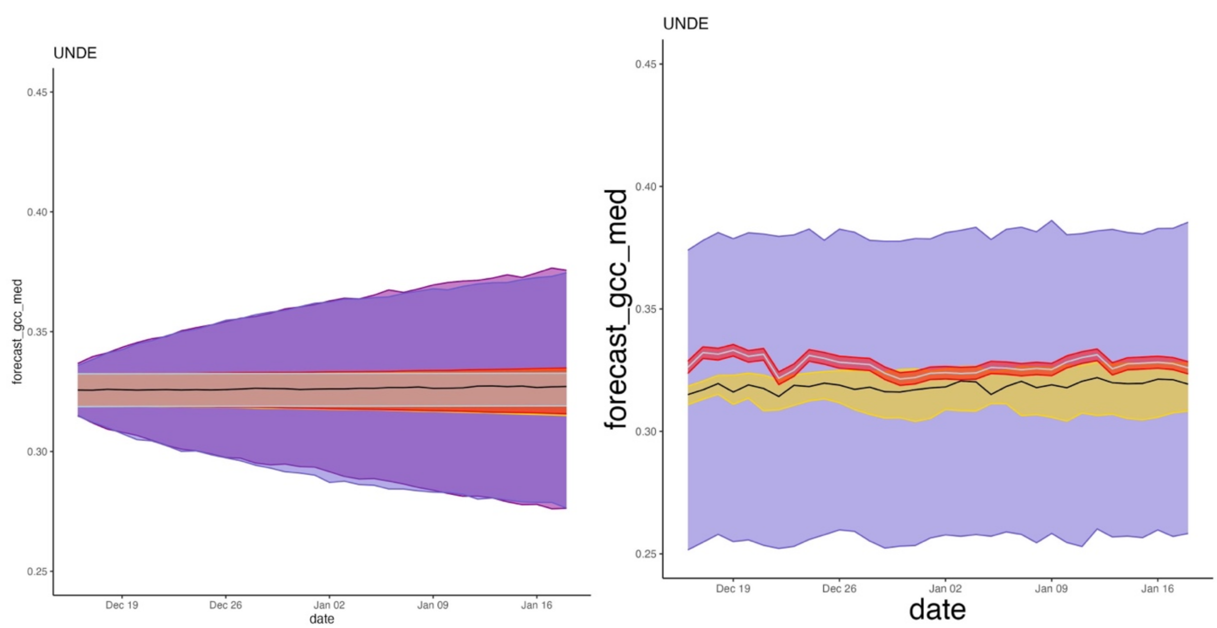

Figure 6: Uncertainty partitioning of RWCD forecast (left) and CD forecast (right) for UNDERC. Light blue represents initial condition uncertainty, red represents parameter uncertainty, yellow represents driver uncertainty, bluish purple represents process uncertainty and reddish purple represents out of site prediction uncertainty.